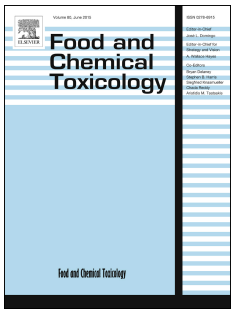

Miquelianin in *Folium Nelumbinis* extract promotes white-to-beige fat conversion *via* blocking AMPK/DRP1/mitophagy and modulating gut microbiota in HFD-fed mice

Zhenyu Wang, Tian Yang, Maomao Zeng, Zhaojun Wang, Qiuming Chen, Jie Chen, Mark Christian, Zhiyong He

PII: S0278-6915(23)00491-X

DOI: https://doi.org/10.1016/j.fct.2023.114089

Reference: FCT 114089

To appear in: *Food and Chemical Toxicology*

Received Date: 17 July 2023

Revised Date: 16 August 2023

Accepted Date: 4 October 2023

Please cite this article as: Wang, Z., Yang, T., Zeng, M., Wang, Z., Chen, Q., Chen, J., Christian, M., He, Z., Miquelianin in *Folium Nelumbinis* extract promotes white-to-beige fat conversion *via* blocking AMPK/DRP1/mitophagy and modulating gut microbiota in HFD-fed mice, *Food and Chemical Toxicology* (2023), doi: https://doi.org/10.1016/j.fct.2023.114089.

Zhenyu Wang: Conceptualization, Investigation, Data curation, Visualization, Writing- Original draft preparation, Software; **Tian Yang**: Investigation, Validation; **Maomao Zeng**: Investigation, Validation; **Zhaojun Wang**: Investigation, Validation; **Qiuming Chen**: Investigation, Validation; **Jie Chen**: Investigation, Validation; **Mark Christian**: Supervision, Writing, Reviewing and Editing; **Zhiyong He**: Conceptualization, Project administration, Supervision, Validation, Writing-review & editing.

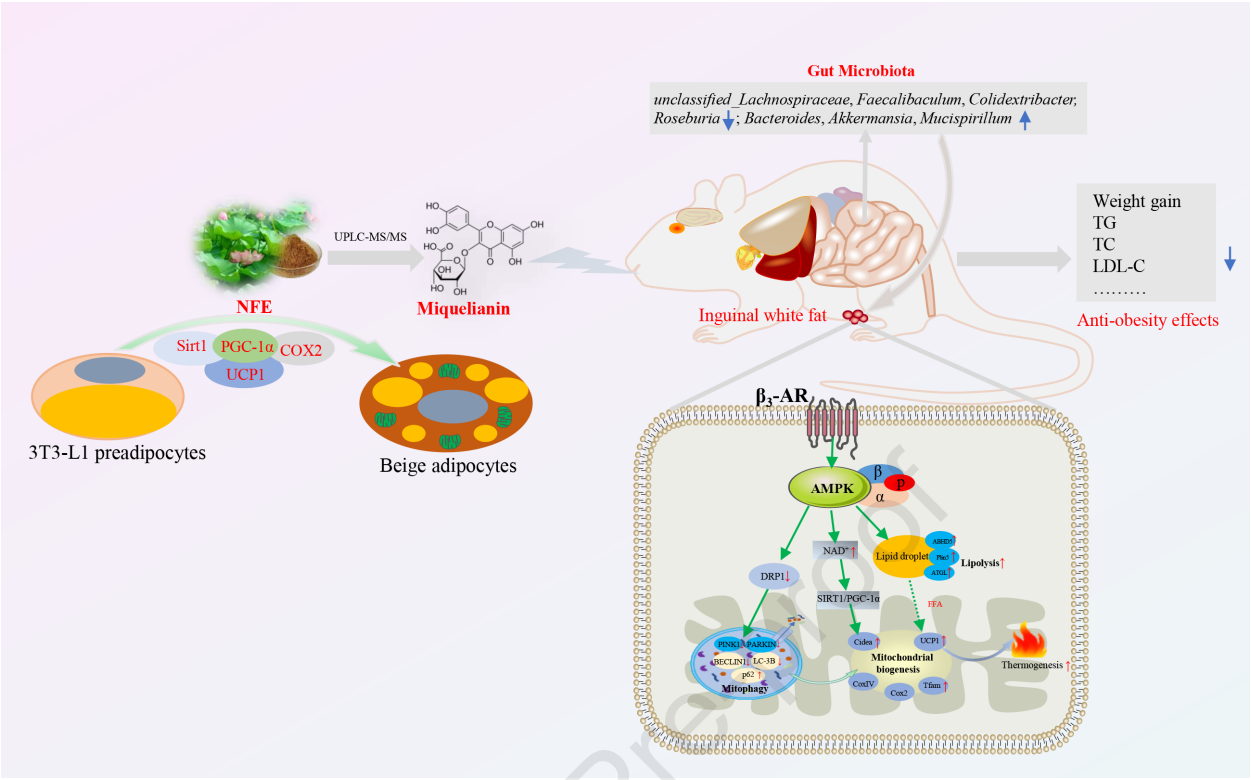

Miquelianin in *Folium Nelumbinis* Extract Promotes White-to-Beige Fat Conversion *via* Blocking AMPK/DRP1/Mitophagy and Modulating Gut Microbiota in HFD-fed mice

Zhenyu Wang [a,b], Tian Yang [a,b], Maomao Zeng [a,b], Zhaojun Wang [a,b], Qiuming Chen [a,b], Jie Chen [a,b], Mark Christian [*,c], and Zhiyong He [*, a,b]

[a]State Key Laboratory of Food Science and Resource, Jiangnan University, Wuxi, Jiangsu 214122, China

[b]International Joint Laboratory on Food Safety, Jiangnan University, Wuxi, Jiangsu 214122, China

[c]School of Science and Technology, Trent University, Clifton, Nottingham, NG11 8NS, United Kingdom

[*]Corresponding author. Tel: +86 510 8591 9065; fax: +86 510 8591 9065.

E-mail address: zyhe@jiangnan.edu.cn (He Z.), mark.christian@ntu.ac.uk (M. Christian)

Abstract

The main purpose of the present study was to investigate the effect of miquelianin (quercetin 3-O-glucuronide, Q3G), one of the main flavonoids in the *Folium Nelumbinis* extract (FNE), on beige adipocyte formation and its underlying mechanisms. In 3T3-L1 adipocytes Q3G (12.8%)-rich FNE treatment upregulated beige-related markers such as SIRT1, COX2, PGC-1α, TFAM, and UCP1. Furthermore, Q3G enhanced mitochondrial biosynthesis and inhibited mitophagy by downregulating the expression of PINK1, PARKIN, BECLIN1 and LC-3B in 3T3-L1 cells. Moreover, in high-fat-diet (HFD)-fed mice, Q3G markedly inhibited body weight gain, reduced blood glucose/lipid levels, reduced white adipose tissues (WAT) and mitigated hepatic steatosis. Meanwhile, the induced beiging accompanied by suppressed mitophagy was also demonstrated in inguinal WAT (iWAT). Chemical intervention of AMPK activity with Compound C (Com C) and Acadesine (AICAR) revealed that AMPK/DRP1 signaling was involved in Q3G-mediated mitophagy and the beiging process. Importantly, 16S rRNA sequencing analysis showed that Q3G beneficially reshaped gut microbiota structure, specifically inhibiting *unclassified_Lachnospiraceae*, *Faecalibaculum*, *Roseburia* and *Colidextribacter* while increasing *Bacteroides*, *Akkermansia* and *Mucispirillum*, which may potentially facilitate WAT beiging. Collectively, our findings provide a novel biological function for *Folium Nelumbinis* and Q3G in the fight against obesity through activating the energy-dissipating capacity of beige fat.

Keywords: Folium Nelumbinis, Miquelianin, Beige fat, Mitophagy, Gut microbiota

1. Introduction

Obesity occurs due to an excess of energy intake over energy expenditure. According to thermodynamic principles, any treatment for obesity requires either reduction in energy intake, or increase in energy expenditure, or both (Tseng, Cypess, & Kahn, 2010). Despite restricting calorie intake as the first line of defense against obesity, changes in metabolic efficiency, such as increasing energy expenditure in adipose tissue or other key metabolic organs, is an important alternative strategy. Studies have found that three types of adipose tissues (white, brown, and beige) exist in mammals with different developmental origins as well as functional and morphological differences (Wang et al., 2023d). White fat stores excess energy as unilocular lipid droplets, but beige adipocytes located in the white adipose tissue (WAT) depots, especially in the subcutaneous area, express more thermogenic and lipolytic genes compared with white adipocytes, which is analogous to brown adipose tissue (BAT), and have attracted increased attention from researchers. Several transcription factors and cofactors, including peroxisome proliferator-activated receptor γ (PPARγ), PR domain-containing 16 (PRDM16), and PPARγ-coactivator-1α (PCG-1α), have been identified as key regulators of white-to-beige adipocyte transdifferentiaiton.

Currently, the “beiging” of white fat is considered a promising treatment for improving metabolic health *via* stimulating non-shivering thermogenesis. A growing body of evidence support that adipose browning/beiging can be induced by external factors (e.g., cold exposure, intermittent fasting, physical exercise) and pharmaceuticals (Wang et al., 2023a). However, these approaches are either

unrealistic (e.g., cold) or risk damage other organs (e.g., thyroid) once the required dose is exceeded. Thus, the search for natural phytochemicals as fat browning/beiging activators is gaining more and more attention due to their safety. *Folium nelumbinis*, the leaves of the lotus (*Nelumbo nucifera* Gaertn.), is produced in excess of 800,000 tons per year and is often discarded as waste, resulting in resource wastage and water contamination (Wang et al., 2021). Actually, as an edible and medicinal resource, *Folium nelumbinis* is rich in nutrients with lipid-lowering and weight-loss effects. The recommended dosages of raw *Folium nelumbinis* for adults are 3-10 g/day according to the national Pharmacopoeia of the People's Republic of China and 30 g/day according to Traditional Chinese medicine formula He-Ye Jiang-Zhi decoction or Shen-He Zhi-Gan (Wang et al., 2016). The predominant bioactive compounds in *Folium nelumbinis* are flavonoids (quercetin and kaempferol derivatives), of which miquelianin (also known as quercetin 3-O-glucuronide (Q3G)) was identified as the most abundant flavonoid (Lee et al., 2020; Qian et al., 2018; Wang et al., 2023b; Ye et al., 2014). *In vitro* and *in vivo* experiments demonstrated that Q3G could combat obesity by inhibiting lipid accumulation in 3T3-L1 adipocytes and enhancing fatty acid oxidation related genes, including ACS1, ACOX1, CPT1b, UCP2 in epididymal adipose tissue of HFD-fed mice (Sim et al., 2019). However, whether these beneficial effects involving adipose beiging remains unknown.

Mitophagy is a fundamental process for maintaining mitochondrial health, and studies support that inhibition of mitophagy by gene knockout or pharmacological interventions facilitate beige adipogenesis and thermogenesis and protects against

insulin resistance and glucose intolerance in high-fat diet (HFD)-induced obese mice (Singh et al., 2009). Furthermore, substantial and compelling evidence from clinical and experimental trials highlights the importance of altered gut microbiota composition and function in enhancing energy expenditure and adipose beiging (Suárez-Zamorano et al., 2015). Here, the beiging effect of *Folium nelumbinis* extract (FNE) was assessed in 3T3-L1 cells and the regulatory mechanism of its major component Q3G was further identified through *in vitro* and *in vivo* experiments. Our findings support that Q3G facilitated beige fat formation by suppressing mitophagy and shifting specific flora components.

2. Materials and Methods

2.1 Materials

Dried *Folium nelumbinis* (Bozhou, Anhui, China) was purchased from Shaanxi Chuliang Agricultural Technology Co., Ltd.. Miquelianin (purity: 99.07%) isolated from the lotus (Nelumbo nucifera) seedpod was purchased from Herbpurify CO., LTD (Chengdu, China). 1-Methyl-3-isobutylxanthine (IBMX), Dexamethasone (Dex), and insulin (Ins) were purchased from Macklin (Shanghai, China).

2.2. Preparation of FNE

Folium nelumbinis extract (FNE) was prepared in accordance with our previous report (Wang et al., 2023b). The content of total polyphenol, total favonoid, total polysaccharide, and protein in FNE were determined to be 383.7 mg/g, 178.3 mg/g, 225.3 mg/g, and 67.3 mg/g, respectively. Seven flavonoids have been identified by

UPLC-MS/MS, with miquelianin (Q3G) being the most abundant, accounting for 12.8 % of the FNE (Wang et al., 2023b).

2.3. Cell culture, differentiation, and treatment

3T3-L1 cells (Chinese Academy of Sciences, Kunming, China) were maintained in DMEM (contains 4.5 g/L D-glucose, L-glutamine, and 110 mg/L sodium pyruvate) with 10% newborn calf serum (Gibco, US) at 37 °C in a 5% CO_2 environment. For differentiation, confluent cells were placed in DMEM containing 10% FBS (Lonsera, Uruguay), 0.5 mM IBMX, 1 mM DEX, and 10 μg/mL Ins for 2 days. Then, the cells were cultured in DMEM containing FNE or Q3G (chemical structure: Fig. 2A) or rosiglitazone (Rosi, 1 μM) and 10 μg/mL of insulin, which was replaced every 2 days until visible lipids appeared (6 days). For AMPK signalling investigations, cells were treated with 5 μM Compond C (Com C) or 10 μM Acadesine (AICAR) (MedChemExpress) on day seven of differentiation and incubated for 24 h, followed by harvesting of cells.

2.4. Cell viability assay

The CCK-8 kit (Beyotime, China) was applied to assess the effects of FNE or Q3G on 3T3-L1 cell viability after 24 hours treatment. The cell viability (%) = (OD_{450} of treated cells-OD_{450} of blank)/(OD_{450} of untreated cells-OD_{450} of blank)×100.

2.5. Bodipy 505/515 lipid staining

Bodipy (green) (1 μM, GLPBIO, USA) was applied to stain for lipid droplets and DAPI (blue) (C1005, Beyotime, China) stained for nuclei, which was consistent with our previous report (Wang et al. 2023a).

2.6. Mitochondrial staining and Mitochondrial membrane potential (MMP)

For the assessment of mitochondrial abundance and membrane potential, the Mitotracker Red and JC-1 probe (Beyotime, China) were used for staining at 37°C for 30 min and assessed by inverted fluorescence microscopy (Axio Vert. A1, Germany). The ratio of aggregate (red) and monomer (green) was used to quantify changes in MMP.

2.7. Dichlorofluorescein assay

1 mL of DCFH-DA (10 μM) was added to cells in the well of a 6-well plate and incubated at 37 °C for 20 min. The stained cells were captured and subsequently analyzed for green fluorescence intensity by Image J.

2.8. Mitophagy assay

To assess mitophagy flux, putative kinase 1 (PINK1)/E3 ubiquitin ligase PARK2 (PARKIN)-mediated mitophagy was induced by FCCP (Strappazzon et al., 2015). 3T3-L1 cells were stimulated by FCCP (10 μM) at 37°C for 1 h, 1 mL of monodansyl cadaverine (MDC) was added and incubated at 37°C for 30 min, followed by capture of microscopy images.

2.9. Animals and experimental diets

Five-week-old male C57BL/6J mice (Beijing Witonglihua Laboratory Animal Technology Co., Ltd., China) were used with the approval of the Animals Center of Jiangnan University (JN.No20220615c1100925[233]). Mice were housed in a 23±1°C environment with a 12:12 hour light-dark cycle, and food and water were freely accessible. After acclimatization for one week, the mice were randomly divided into

five groups (n=8): normal diet (ND, consisted of fat 10%, carbohydrate 71.0%, protein 19.0%) group, high-fat diet (HFD, consisted of fat 60%, carbohydrate 20.6%, protein 19.4%) group, Q3G-L (HFD plus 12.8 mg/kg of Q3G) group, Q3G-H (HFD plus 25.6 mg/kg of Q3G) group, and MI (HFD plus 5mg/kg of miglitol) group. All samples were dissolved in 0.5% CMC-Na and mice were gavaged orally once/day.

2.10. Measurement of blood glucose, serum biochemical parameters and body temperature

One week before the experiment ended, blood was taken from the tail vein of the different groups of mice after 12 hours of fasting and the fasting blood glucose (FBG) levels were measured using a glucometer (Roche Accu-Chek Go). After the 12-week feeding regime, mice were sacrificed after being fasted for 12 hours, and whole blood was obtained by removing the eyeball and centrifuged at 4000 rpm for 10 minutes at 4℃. The triglycerides (TG), total cholesterol (TC), high-density lipoprotein cholesterol (HDL-C) and low-density lipoprotein cholesterol (LDL-C) in serum were assayed as described in the assay kit (Nanjing Jiancheng Bioengineering institute, Nanjing, China).

2.11. Histopathological analysis

Paraformaldehyde-fixed tissues, including eWAT (epididymal WAT), iWAT (inguinal WAT), and liver were embedded in paraffin and 5 μm thick slices were sectioned. Pathological analysis was conducted upon hematoxylin and eosin (H&E) staining.

2.12. Quantitative RT-PCR and immunoassay

The total RNA extraction, cDNA synthesis, and qPCR were performed following our

previous studies (Wang et al. 2023b). The primer sequences are listed in Supplemental Table 1. Immunohistochemistry and immunofluorescence of UCP1 and SIRT1 were performed following the protocol of the PV9000 immunohistochemistry kit (Servicebio, Wuhan, China) as described previously (Liu et al., 2022). Immunoblotting was carried out in agreement with our previous study (Wang et al. 2023b). Primary antibodies, including (p)AMPKα, (p)AMPKβ1, (p)ACC, UCP1, ATGL, ABHD5, PLIN5, SIRT1, PGC-1α, TFAM, NAMPT, COX-2, COX-IV, DRP1, PINK1, PARKIN, BECLIN1, LC-3B, and DRP1 (1:1000, Proteintech), p-DRP1$_{Ser637}$ (1:1000, Affinity), and β_3-AR (1:1000, Abclonal) were used for protein expression assay. β-actin, β-tubulin, or GAPDH expression was used as internal loading controls.

2.13. 16S rRNA gene sequencing

Cecum samples were collected in sterile lyophilized tubes and microbial DNA was extracted using the the Omega DNA Kit following the manufacturer's instructions. The subsequent procedures were carried out as previously described (Mu et al., 2021) and are detailed in the supplementary material.

2.14. Statistical analysis

Data from individual experiments are presented as means ± standard deviation. Statistical significance was calculated using one-way analysis of variance with Duncan's test. Values of $p<0.05$ were considered to be statistically significant.

3. Results

3.1. FNE potentially induces beiging of 3T3-L1 adipocytes

We first assessed whether FNE could induce beiging of 3T3-L1 adipocytes. Based on the results of CCK-8 assay, 100 and 200 μg/mL of FNE were selected for investigation in 3T3-L1 adipocytes (Fig. 1A). The mRNA expression of beige-related genes (*Sirt1*, *Ppargc1a*, *Tfam* and *Ucp1*) was significantly upregulated in the FNE group as compared to the control (Fig. 1B). Moreover, the expression of the proteins SIRT1, COX2, and UCP1 was also upregulated (Fig. 1C and 1D). Immunofluorescence also showed higher abundance of SIRT1 and UCP1 in FNE-treated cells (Fig. 1E and 1F). The above results suggest FNE's potential action on adipocyte beiging. Since FNE contains high levels of Q3G (12.8%), we hypothesized that Q3G may function in the FNE-induced beiging, and therefore we focused on the effect of Q3G in the subsequent experiments.

3.2. Q3G promotes lipolysis during the differentiation of 3T3-L1 cells

As observed in Fig. 2B, Q3G stimulation for 24 h had no significant cytotoxic effect on 3T3-L1 cells. Q3G (5 and 10 μM) was found to reduce lipid droplet accumulation similar to Rosi (1 μM) through neutral Bodipy 505/515 fluorescent dye staining (Fig. 2C and 2D). There was marked increased in protein expressions of lipolytic markers, including adipose triglyceride lipase (ATGL), abhydrolase domain containing 5 (ABHD5), and Perilipin 5 (PLIN5) in Q3G-treated cells with effects comparable to those of positive controls (Rosi) (Fig. 2E and 2F).

3.3. Q3G enhances mitochondrial activity in 3T3-L1 cells

Mitochondrial function has been shown to be a major determinant of functional lipid storage and oxidation, which is of particular relevance for brown/beige adipocytes.

The effects of Q3G on mitochondrial function were investigated. Mito-Tracker Red staining revealed increased density presented in the Q3G-treated cells indicated that Q3G enhanced mitochondrial activity (Fig. 2G and 2J). In line with this, a significant decrease in ROS content was also found in Q3G-treated 3T3-L1 cells compared with untreated cells (Fig. 2H and 2K). Furthermore, assessment of the MMP by JC-1 fluorescence demonstrated Q3G treatment enhanced MMP, evidenced by the reduction in monomer (green) and increase in aggregate (red) (Fig. 2I and and 2L). Taken together, these findings demonstrate that Q3G facilitates an improvement of mitochondrial activity in 3T3-L1 cells.

3.4. Q3G induces beiging and mitochondrial biogenesis in 3T3-L1 cells

As shown in Fig. 3A-C, Q3G stimulation upregulated mRNA (e.g., *Tfam*, *Cox2*, *Cox-IV*, and *Pparα*) and protein (TFAM and COX-IV) expression levels of mitochondrial biogenesis-associated markers. In support of this, a higher relative mRNA expressions of beige-fat-enriched genes (e.g., *Ucp1*, *Ppargc1a*, *Prdm16*, *Sirt1*, *Cd40*, *Cited1*, and *Fgf21*) were exhibited in Q3G-treated cells compared with the untreated control. In addition, Western blot analyisis confirmed that Q3G dose-dependently augmented the protein expression of UCP1, PGC-1α, SIRT1 and NAMPT (Fig. 3B and 3C). Immunofluorescence also showed increased staining for SIRT1 and UCP1 (Fig. 3D and 3E). Importantly, the protein expression of β_3-AR and its downstream targets AMPKα/β1 and ACC was significantly induced by Q3G, with results comparable to those of the Rosi group (Fig. 3F and 3G).

3.5. Q3G improves mitochondrial quality by suppressing mitophagy in 3T3-L1

cells

Autophagy is also considered as an important factor in evaluating mitochondrial quality. Mitochondrial biogenesis works in combination with mitophagy to maintain mitochondrial homeostasis (Lu et al., 2018). Mitophagy suppression was observed in FCCP and Q3G co-treated 3T3-L1 cells compared with FCCP-stimulated 3T3-L1 cells using Mtphagy dye (Fig. 4A and 4B). qPCR results showed that Q3G (especially 10μM) treatment significantly reduced expression of autophagy-promoting genes (e.g., *Pink1*, *Parkin*, *LC3B*, and *Beclin1*) and upregulated p62 expression (an adaptor degrading autophagosome) (Fig. 4C). Further results were also confirmed by Western blot (Fig. 4D and 4E). We also found the expression of mitochondrial fission-associated protein p-DRP1 was increased in Q3G-treated cells.

3.6. Effects of Q3G on body parameters and blood biochemical indexes in HFD-fed mice

As shown in Fig. 5, the HFD group exhibited a significant trend towards body weight gain (BG) (Fig. 5A), liver/body weight (Fig. 5C), eWAT/body weight (Fig. 5D), and iWAT/body weight (Fig. 5E) relative to the control group. However, Q3G administration reversed these changes in a dose-dependent manner, approaching the positive control MI group. Importantly, we found no significant differences in food intake (Fig. 5B) among the different groups of mice. The results of blood biochemical indicators tests showed that Q3G supplementation dose-dependenly reversed the HFD-induced increase in TG, TC, LDL-C, and FBG levels and decreased HDL-C levels (Fig. 5F-J). The effects were very similar to the MI treatment group. The above

results suggest that Q3G supplementation significantly inhibited body weight gain and improved glycolipid levels in HFD-fed mice without affecting their food intake.

3.7. Effects of Q3G on the histopathology in HFD-fed mice

As shown in Fig. 5, Q3G treatment significantly reduced adipocyte size within eWAT (Fig. 5K and 5O) and iWAT (Fig. 5I and Fig. 5P) and reached a similar level to the MI group, implying that Q3G may promote lipid consumption in adipocytes. We histopathologically sectioned the liver and kidney of mice, and the results revealed that the liver of HFD-fed mice showed significant steatosis with large amounts of lipid deposition compared to the ND group. In contrast, the liver in the Q3G-treated group showed lower NAFLD activity score (NAS devised by NASH CRN) (Kleiner et al., 2005) (Fig. 5M and 5Q). Furthermore, the kidney of Q3G-treated mice showed no significant injury and was similar to the ND group (Fig. 5N).

3.8. Q3G indues beiging of iWAT in HFD-fed mice

The results in iWAT showed Q3G treatment dose-dependently upregulated the expression of beige fat-related genes (e.g., *Sirt1*, *Ppargc1a*, *Prdm16*, *Cidea*, *Dio2*, *Nrf1*, *Tfam*, *Ucp1*, *Cox2*, *Pparα*, *Cited1*, *Fgf21*, *Tbx1*, and *Cd40*) (Fig. 6A). In addition, the higher expression of SIRT1 and UCP1 was also demonstrated by immunofluorescence (Fig. 6B). The significant increase in protein expression of β_3-AR, SIRT1, PGC-1α, COX2, TFAM, ABHD5, and UCP1 as well as the ratio of p-AMPKα/AMPKα upon Q3G were confirmed by Western blot (Fig. 6C).

3.9. Q3G inhibited mitophagy and induced beiging *via* AMPK/DRP1 signaling

Western blot analysis of iWAT showed that Q3G treatment also dose-dependently

downregulated the expression of autophagy-promoting proteins (e.g., PINK1, PARKIN, BECLIN1, and LC3B) and upregulated autophagy adaptor protein p62 in Q3G-treated iWAT compared with the HFD group (Fig. 7A and 7B), suggesting the inhibitory effect of Q3G on mitophagy. Moreover, Q3G also was found to inhibit the activity of DRP1 by phosphorylating at position ser637 (Fig. 7A and 7B). Subsequently, Com C and AICAR were added to identify the involvement of AMPK signaling in Q3G-regulated DRP1/mitophagy and the beiging process. Immunostaining staining of UCP1 revealed pretreatment with Com C inhibited Q3G-induced increase but AICAR reversed the trend (Fig. 7C). The results of Western blot showed Com C suppressed Q3G-stimulated upregulation of mitofission protein p-DRP1 and beige-fat-related markers SIRT1, PGC-1α, COX-2, and UCP1. Furthermore, Com C reversed or blunted the downregulation of autophagy proteins PINK1, PARKIN, BECLIN1, and LC-3B instigated by Q3G (Fig. 7D and 7E). AICAR in contrast to Comp C largely caused further upregulation of mitofission protein (p-DRP1) and brown-fat-enriched markers (SIRT1, PGC-1α, COX-2, and UCP1), and downregulation of autophagy proteins (PINK1, PARKIN, BECLIN1, and LC-3B) compared to Q3G alone (Fig. 7D and 7E).

3.10. Q3G remodels the gut microbiome in response to HFD

It is likely that orally administered Q3G was not completely absorbed due to its low bioavailability and would reach the colon. Subsequently, it could be utilized by gut microbes and thus indirectly affect the host metabolism. To investigate whether Q3G treatment altered the gut microbiota, 16S rRNA gene sequencing analysis was

performed. An average of 262, 146, 199, and 239 OTUs were identiffed in the ND, HFD, Q3G-L, and Q3G-H groups, respectively (Fig. 8A). Apha diversity analysis showed that Q3G had no significant effect on the Shannon index (Fig. 8B) but reduced the Chao1 index (Fig. 8C), suggesting that Q3G treatment failed to affect the microbial diversity in HFD-fed mice but reduced the species number. Moreover, the non-metric multidimensional scaling (NMDS) analysis revealed that the compositions of the gut microbiota in the ND, HFD, Q3G-L and Q3G-H groups had their own distinct cluster (Fig. 8D). The data from taxonomic analysis at the phylum level indicates Q3G-H treatment significantly reduced *Firmicutes* phylum without affecting *Bacteroidota* richness (Fig. 8E). Correspondingly, the ratio of *Firmicutes/Bacteroidota* (F/B) in Q3G-H-treated mice showed a decreased trend but without statistical difference compared to that in the HFD group (Fig. 8E(3)). At the family level, the lower *Lachnospiraceae* and higher *Bacteroidaceae* and *Akkermansiaceae* abundance have been observed in Q3G-H-treated mice than in the HFD group (Fig. 8F). The LEfSe (LDA>3) assay showed that in total 45 different OTUs, including 1 phyla and 19 genera, were found as key phylotypes in the ND and HFD groups; in total 45 different OTUs, including 1 phyla and 19 genera, were found as key phylotypes in the ND and HFD groups (Fig. 8G); in total 36 different OTUs, including 1 phyla and 18 genera, were found as key phylotypes in the HFD and Q3G-L groups (Fig. 8H); in total 34 different OTUs, including 1 phyla and 15 genera, were found as key phylotypes in the HFD and Q3G-H groups (Fig. 8I). Given that genus-level assignment of bacteria performs great functional roles, the top 20 genera are

shown in Fig. 8J. Compared to ND group, the abundance of *unclassified_Lachnospiraceae*, *Lachnospiraceae_NK4A136_group*, *Colidextribacter*, *Faecalibaculum, and Roseburia* were enriched, whereas *unclassified_Muribaculaceae*, *Blautia*, *Bilophila*, and *Oscillibacter* were lower in HFD group. Furthermore, compared to the HFD group, Q3G-H reduced unclassified_*Lachnospiraceae*, *Faecalibaculum*, and *Roseburia*, whereas it increased *Bacteroides*, *Akkermansia*, *Mucispirillum*, and *Blautia*. Spearman's correlation analysis showed *Akkermansia*, *Bacteroi*des, and *Mucispirillum* were positively correlated with beige fat-related markers, whereas unclassified_*Lachnospiraceae*, *Colidextribacter*, *Roseburia* and *Faecalibaculum* were negatively correlated with beige fat-related markers (p<0.05) (Fig. 8K). Additionally, *unclassified_Lachnospiraceae* and *Colidextribacter* showed a positive relationship with obesity-related indicators (e.g., BG, TC, LDL-C), whereas *Faecalibaculum* and *Bilophila* showed a negative relationship with obesity-related indicators (e.g., TC, LDL-C) (p<0.05).

4. Discussion

The beiging of WAT provides a defense against diet-induced obesity and the associated metabolic disorders. Natural compounds that induce beiging of white adipocytes are an attractive potential strategy to fight obesity. Numerous studies have reported that *Folium nelumbini*s can combat obesity, but little has been reported regarding the beiging mechanism. Investigation in 3T3-L1 cells demonstrated that FNE induced brown-like adipocyte formation. UPLC-MS/MS analysis of FNE

showed that Q3G was the main flavonoid and may be responsible for FNE-induced beiging, thus warranting further investigation.

MMP is considered an important indicator of mitochondrial function; high MMP value implies high mitochondrial activity, and increased mitochondrial reactive oxygen species is positively associated with abrogation or inhibition of UCP1 (Liu et al., 2019). The redox coupling of NAD^+/NADH greatly determines the homeostasis of mitochondrial metabolism (Jia et al., 2022). Here, we observed that expression of the rate-limiting NAD^+ biosynthesis enzyme NAMPT expression and NAD^+ content were significantly enhanced in Q3G-treated cells, which were in agreement with a previous study that observed increased NAD^+ levels during beige adipogenesis (Jia et al., 2022). β_3-AR/AMPK signaling has been reported to be responsible for the formation and maintenance of brown and beige adipocytes, and it regulates mitochondrial biogenesis (e.g., Nrf family, Tfam, and PPARs) by signaling through PGC-1α and enhancing SIRT1 activity via upregulation of cellular NAD^+ levels (Jang et al., 2018; Kang et al., 2018). In 3T3-L1 cells, the beige-fat-phenotype has been induced by quercetin treatment *via* β_3-AR/AMPKα signaling (Kong et al., 2022). Our previous work in $C_3H_{10}T_{1/2}$ cells also demonstrated that Q3G induced SIRT1, PGC-1α, and UCP1 expression through activation of β_3-AR/AMPK during brown adipocyte differentiation (Wang et al. 2023c). Here, increased β_3-AR activity and AMPK phosphorylation accompanied by upregulated mitochondrial biosynthesis-related factors were also observed in 3T3-L1 cells and iWAT, supporting the possibility that β3-AR/AMPK signaling may be involved in Q3G-regulated adipocyte beiging.

Mitophagy can work in combination with mitochondrial biogenesis to maintain mitochondrial homeostasis (Park et al., 2018). Many pharmacological agents have been shown to lower mitophagy in beige adipocytes to stimulate mitochondrial and thermogenic programing (Lu et al., 2018). Studies have shown that liensinine and raspberry ketone can inhibit the conversion of beige adipocytes into a white phenotype and maintain the beige-like features by mitophagy suppression (Leu et al., 2018; Xie et al., 2019). PINK1 and PARKIN work together to induce selective autophagy as a key regulator of brown or beige-fat-phenotype (Rahman & Kim, 2020). In Rosi treated 3T3-L1 adipocytes and CL 316,243 (a β_3-adrenoceptor agonist)-treated iWAT, markedly lowered PARKIN expression, a marker of mitochondria targeted for degradation, was observed, but UCP1 was strongly induced, indicating that WAT beiging correlates with decreased PARKIN-mediated mitophagy (Taylor & Gottlieb, 2017). In line with this study, sesamol was considered to promote beiging and mitochondrial biogenesis in 3T3-L1 cells by inhibiting mitophagy (Lin et al., 2021). Previous reports evidence that autophagic vacuole structures present in high-glucose (20mM)-induced 3T3-L1 adipocytes can be recovered by Q3G (Herranz-López et al., 2020). Importantly, in $C_3H_{10}T_{1/2}$-induced differentiation into brown adipocytes, we also observed that Q3G reduced mitophagy by transmission electron microscopy, qPCR, and western blotting (Wang et al., 2023b). Here, the suppression of PINK1-PARKIN regulated mitophagy was confirmed in Q3G-treated 3T3-L1 cells and iWAT of HFD-fed mice, indicating the potential of Q3G-meditated mitophagy in adipocyte beiging.

DRP1 is a major regulator of mitochondrial dynamics and its inhibition could reverse the downregulation of MMP and diminish mitochondrial fission under high glucose conditions (Zhang et al., 2022). In isolated WAT adipocytes from ob/ob mice, DRP1 blockade was found to induce white-to-beige adipocyte transdifferentiation. In ob/ob mice, inhibition of DRP1 by mdivi-1 induced p-AMPK, PGC-1α and UCP1 expression and increased mitochondrial mass in WAT, suggesting the importance of DRP1 inhibition in WAT beiging (Finocchietto et al., 2022). Moreover, DRP1 has been found as a PARKIN and PINK1 enhancer (Poole et al., 2008), and the suppression of its activity decreased PINK, PARKIN, and LC3II expression and translocation to mitochondria (Park et al., 2018; Tanaka et al., 2010). The same phenomenon of DRP1 silencing/knockdown that inhibits mitophagy has also been found in other cells (Buhlman et al., 2014; Pernaute et al., 2022; Wu et al., 2022). Evidence suggests a positive relation between AMPK phosphorylation and inhibition of DRP1 in WAT (Finocchietto et al., 2022). Activation of AMPK can downregulate DRP1 expression by phosphorylating DRP1 at serine 637, which then suppresses mitophagy and recruitment of PARKIN to mitochondria for the formation of mitochondrial autophagosomes (Herzig & Shaw, 2018; Li et al., 2015). In high glucose (33 mM)-stimulated 3T3-L1 cells, it has been found that metformin or resveratrol activated AMPK, phosphorylated DRP1 at Ser637, and prevented mitochondrial fission during 8-10 days of differentiation, but knockdown of AMPKα blocked their action in restoring DRP1 phosphorylation (Ser 637), indicating the potential role of AMPK/DRP1 signaling in mitochondrial fission (Li et al., 2016).

Consistent with the above studies, activation of AMPK was accompanied with upregulated DRP1 phosphorylation (Ser637), inhibited mitophagy, and enhanced mitochondrial biogenesis in 3T3-L1 cells and iWAT, suggesting that Q3G induced beiging through AMPK/DRP1/mitophagy signaling.

Recently, substantial research has revealed a metabolic interaction between the gut microbial communities and the host, with emerging evidence that specific bacteria may be involved in the remodeling of WAT toward a beige phenotype in obese patients (Wang, et al., 2023d). *Firmicutes* and *Bacteroidetes* were the main microbiota phylum of obese animals with subjects showing high abundance of *Firmicutes* and low abundance of *Bacteroidetes* (Ley et al., 2006). However, there is controversy regarding alteration of the F/B ratio in obesity, with some studies not observing any change in this parameter and even reporting a decrease in the F/B ratio in obese animals and humans (Magne et al., 2020). Thus, variations in specific components exist at sub-levels (e.g., family, genus) that may be more relevant than the F/B ratio. *Lachnospiraceae* (*Firmicutes* phylum) was enriched in obesity subjects and a correlation analysis revealed *unidentified_Lachnospiraceae* at the genus level positively associated with obesity-related indices (BG, TG, TC, and LDL-C) and negatively associated with leptin, HSL and UCP1 expression in WAT (Kang et al., 2022). The *Colidextribacter* spp. (*Firmicutes* phylum) was proposed as an HFD-dependent taxa, and some functional components such as flavonoids can modulate HFD-induced perturbation of *Colidextribacter* (Wu et al., 2022). Consistent with these findings, *unidentified_Lachnospiraceae* and *Colidextribacte* showed positive

correlation to obesity-related traits and negative correlation to beige-related markers, but Q3G reversed their HFD-induced increase. *Bacteroides* spp. (*Bacteroidetes* phylum) was considered due to their production of bile acids (e.g, lithocholic acid) and short-chain fatty acids (SCFAs) and investigations in HFD-fed mice revealed that intragastrically administered *Bacteroides* spp. (*B. dorei* and *B. vulgatus*) could inhibit body weight gain, enhance body temperature, and induce UCP1 expression in HFD-fed mice (Yoshida et al., 2021). Furthermore, *Akkermansia* spp. (*Verrucomicrobia* phylum) candidate probiotic for improving obesity, and substantial animal studies have highlighted its role as a key SCFAs producer that modulates adipose tissue composition, specifically beiging of WAT (Koh et al.; Wang et al., 2023d). The transplantation of *Akkermansia*-rich fecal bacteria has been found to trigger beige adipocyte appearance *via* leptin-mediated AMPKα signaling, but the depletion of the microbiota by antibiotics eliminated this adipose remodeling (Xu et al., 2020). In line with these results, a positive relationship was observed between these two genera (*Bacteroides* spp. and *Akkermansia* spp.) and expression of beige fat-related markers (e.g., *Ppargc1a*, *Nrf1*, *Ucp1*, *Sirt1*, and *Cox2*) in our study, supporting their contribution to beiging. Moreover, integrated analysis of metagenomics and metatranscriptome sequencing data indicates that *Mucispirillum* spp. (phylum *Deferribacteres*) is closely involved in energy metabolism, especially metabolism related to mitochondria. The mechanism by which the flora affects adipose tissue may be strongly linked to its production of metabolites (e.g, free fatty acids, SCFAs) (Chen et al., 2022). This is in line with our data where a positive association between

Mucispirillum spp. abundance and elevated beige and mitochondria-related markers (e.g., *Ppargc1a*, *Sirt1*, *Ucp1*, *Nrf1*, *Pparα*, *Cox2*, *Fgf21*, and *Cited1*) in iWAT was observed. Collectively, Q3G-induced alterations in the above specific flora may be responsible for weight loss and adipose beiging, but requires further identification, e.g., by means of fecal transplants or germ-free mice.

5. Conclusions

Miquelianin, the main flavonoid in *Folium Netlumbinis*, could stimulate WAT beiging in 3T3-L1 cells and iWAT of HFD-fed mice. The potential mechanisms associated with the inhibition of AMPK/DRP1/mitophagy and remodeling of gut microbiota profile (Fig. 9). Our findings shed new light on the use of *Folium Nelumbinis* to ameliorate obesity and point to the potential of miquelianin as a novel food ingredient or nutritional element with the potential to enhance energy dissipation.

Declarations of competing interest

The authors declare no conflicts of interest.

Acknowledgments

The authors acknowledge financial support from the National Key Research and Development Program of China (No. 2022YFF1100204), the National Natural Science Foundation of China (No. 31771978), and the Six Talent Peaks Project in Jiangsu Province (No. NY-095).

References

Buhlman, L., Damiano, M., Bertolin, G., Ferrando-Miguel, R., Lombès, A., Brice, A., Corti, O., 2014. Functional interplay between Parkin and Drp1 in mitochondrial fission and clearance. BBA-Mol Cell Res, 1843 (9), 2012-2026.

Chen, S., Xu, M., Zhou, M., He, Y., Li, Y., Lang, H., Wei, X., Yan, L., Xu, H., 2022. Hibiscus manihot L improves obesity in mice induced by a high-fat diet. J. Funct. Foods 89, 104953.

Finocchietto, P., Perez, H., Blanco, G., Miksztowicz, V., Marotte, C., Morales, C., Peralta, J., Berg, G., Poderoso, C., Poderoso, J., Carreras M., 2022. Inhibition of mitochondrial fission by Drp-1 blockade by short-term leptin and Mdivi-1 treatment improves white adipose tissue abnormalities in obesity and diabetes. Pharmacol. Res. 178, 106028.

Herranz-López, M., Olivares-Vicente, M., Rodríguez Gallego, E., Encinar, J. A., Pérez-Sánchez, A., Ruiz-Torres, V., Joven, J., Roche, E., Micol, V., 2020. Quercetin metabolites from Hibiscus sabdariffa contribute to alleviate glucolipotoxicity-induced metabolic stress in vitro. Food Chem. Toxicol.144, 111606.

Herzig, S., Shaw, R. J. 2018., AMPK: guardian of metabolism and mitochondrial homeostasis. Nat. Rev. Mol. Cell Biol. 19 (2), 121-135.

Jang, M. H., Kang, N. H., Mukherjee, S., Yun, J. W., 2018. Theobromine, a Methylxanthine in Cocoa Bean, Stimulates Thermogenesis by Inducing White Fat Browning and Activating Brown Adipocytes. Biotechnol. Bioprocess Eng. 23 (6), 617-626.

Jia, R., Wei, X., Jiang, J., Yang, Z., Huang, J., Liu, J., Yan, J., Luo, X., 2022. NNMT is induced dynamically during beige adipogenesis in adipose tissues depot-specific manner. J. Physiol. Biochem. 78 (1), 169-183.

Kang, N. H., Mukherjee, S., Min, T., Kang, S. C., Yun, J. W., 2018. Trans-anethole ameliorates obesity via induction of browning in white adipocytes and activation of brown adipocytes. Biochimie 151, 1-13.

Kang, Y., Kang, X., Yang, H., Liu, H., Yang, X., Liu, Q., Tian, H., Xue, Y., Ren, P., Kuang, X., Cai, Y., Tong, M., Li, L., Fan, W., 2022. Lactobacillus acidophilus ameliorates obesity in mice through modulation of gut microbiota dysbiosis and intestinal permeability. Pharmacol. Res. 175, 106020.

Kleiner, D. E., Brunt, E. M., Van Natta, M., Behling, C., Contos, M. J., Cummings, O. W., Ferrell, L. D., Liu, Y. C., Torbenson, M. S., & Unalp-Arida, A. J. H., 2005. Design and validation of a histological scoring system for nonalcoholic fatty liver disease. Hepatology 41 (6), 1313-1321.

Koh, Y.-C., Lin, S.-J., Hsu, K.-Y., Nagabhushanam, K., Ho, C.-T., Pan, M.-H., 2023 Pterostilbene Enhances Thermogenesis and Mitochondrial Biogenesis by Activating the SIRT1/PGC-1α/SIRT3 Pathway to Prevent Western Diet-Induced Obesity. Mol. Nutr. Food Res. 2300370.

Kong, L., Zhang, W., Liu, S., Zhong, Z., Zheng, G., 2022. Quercetin, Engelitin and Caffeic Acid of Smilax china L. Polyphenols, Stimulate 3T3-L1 Adipocytes to Brown-like Adipocytes Via β3-AR/AMPK Signaling Pathway. Plant Foods

Hum. Nutr. 77 (4), 529-537.

Lee, J. S., Paje, L. A., Choi, W.-H., Cho, E. J., Kim, H. Y., Jacinto, S. D., Lee, S. J. A. B. C., 2020. Validation of an optimized HPLC/UV method for the quantification of flavonoids in lotus. Appl. Biol. Chem. 63, 1-6.

Leu, S.-Y., Tsai, Y.-C., Chen, W.-C., Hsu, C.-H., Lee, Y.-M., Cheng, P.-Y., 2018. Raspberry ketone induces brown-like adipocyte formation through suppression of autophagy in adipocytes and adipose tissue. J. Nutr. Biochem. 56, 116-125.

Ley, R. E., Turnbaugh, P. J., Klein, S., Gordon, J. I., 2006. Human gut microbes associated with obesity. Nature 444 (7122), 1022-1023.

Li, A., Zhang, S., Li, J., Liu, K., Huang, F., Liu, B., 2016. Metformin and resveratrol inhibit Drp1-mediated mitochondrial fission and prevent ER stress-associated NLRP3 inflammasome activation in the adipose tissue of diabetic mice. Mol. Cell. Endocrinol. *434*, 36-47.

Li, J., Wang, Y., Wang, Y., Wen, X., Ma, X. N., Chen, W., Huang, F., Kou, J., Qi, L. W., Liu, B., Liu, K., 2015. Pharmacological activation of AMPK prevents Drp1-mediated mitochondrial fission and alleviates endoplasmic reticulum stress-associated endothelial dysfunction. J. Mol. Cell. Cardiol 86, 62-74.

Lin, C., Chen, J., Hu, M., Zheng, W., Song, Z., Qin, H., 2021. Sesamol promotes browning of white adipocytes to ameliorate obesity by inducing mitochondrial biogenesis and inhibition mitophagy via β3-AR/PKA signaling pathway. Food Nutr. Res. 65.

Liu, C., Gao, W., Zhao, L., Cao, Y., 2022. Progesterone attenuates neurological deficits and exerts a protective effect on damaged axons via the PI3K/AKT/mTOR-dependent pathway in a mouse model of intracerebral hemorrhage. Aging 14 (6), 2574-2589.

Liu, M., Zheng, M., Cai, D., Xie, J., Jin, Z., Liu, H., Liu, J., 2019. Zeaxanthin promotes mitochondrial biogenesis and adipocyte browning via AMPKα1 activation. Food Funct. 10 (4), 2221-2233.

Lu, X., Altshuler-Keylin, S., Wang, Q., Chen, Y., Henrique Sponton, C., Ikeda, K., Maretich, P., Yoneshiro, T., Kajimura, S., 2018. Mitophagy controls beige adipocyte maintenance through a Parkin-dependent and UCP1-independent mechanism. Sci. Signaling 11 (527).

Lu, Y., Fujioka, H., Joshi, D., Li, Q., Sangwung, P., Hsieh, P., Zhu, J., Torio, J., Sweet, D., Wang, L., Chiu, S. Y., Croniger, C., Liao, X., Jain, M. K., 2018. Mitophagy is required for brown adipose tissue mitochondrial homeostasis during cold challenge. Sci. Rep. 8 (1), 8251.

Magne, F., Gotteland, M., Gauthier, L., Zazueta, A., Pesoa, S., Navarrete, P., Balamurugan, R., 2020. The Firmicutes/Bacteroidetes Ratio: A Relevant Marker of Gut Dysbiosis in Obese Patients? Nutrients 12 (5), 1474.

Mu, H.-N., Zhou, Q., Yang, R.-Y., Tang, W.-Q., Li, H.-X., Wang, S.-M., Li, J., Chen, W.-X., Dong, J., 2021. Caffeic acid prevents non-alcoholic fatty liver disease induced by a high-fat diet through gut microbiota modulation in mice. Food Res. Int. 143, 110240.

Park, Y. S., Choi, S. E., Koh, H. C., 2018. PGAM5 regulates PINK1/Parkin-mediated mitophagy via DRP1 in CCCP-induced mitochondrial dysfunction. Toxicol. Lett. 284, 120-128.

Pernaute, B., Pérez-Montero, S., Sánchez Nieto, J. M., Di Gregorio, A., Lima, A., Lawlor, K., Bowling, S., Liccardi, G., Tomás, A., Meier, P., Sesaki, H., Rutter, G. A., Barbaric, I., Rodríguez, T. A., 2022. DRP1 levels determine the apoptotic threshold during embryonic differentiation through a mitophagy-dependent mechanism. Dev. Cell 57 (11), 1316-1330.e1317.

Poole, A. C., Thomas, R. E., Andrews, L. A., McBride, H. M., Whitworth, A. J., Pallanck, L. J., 2008. The PINK1/Parkin pathway regulates mitochondrial morphology. Proc. Natl. Acad. Sci. USA 105 (5), 1638-1643.

Qian, Y., Chen, X., Qi, J., Liu, X., 2018. A novel analytical method based on HPLC-PDA coupled post-column derivatization to evaluate the ability to inhibit tyrosine nitration in lotus leaf extracts. RSC advances 8 (68), 38715-38720.

Rahman, M. S., & Kim, Y.-S. (2020). PINK1–PRKN mitophagy suppression by mangiferin promotes a brown-fat-phenotype via PKA-p38 MAPK signalling in murine C3H10T1/2 mesenchymal stem cells. Metabolism 107, 154228.

Sim, W.-S., Choi, S.-I., Cho, B.-Y., Choi, S.-H., Han, X., Cho, H.-D., Kim, S.-H., Lee, B.-Y., Kang, I.-J., Cho, J.-H., Lee, O.-H., 2019. Anti-Obesity Effect of Extract from Nelumbo Nucifera L., Morus Alba L., and Raphanus Sativus Mixture in 3T3-L1 Adipocytes and C57BL/6J Obese Mice. Foods 8 (5), 170.

Singh, R., Xiang, Y., Wang, Y., Baikati, K., Cuervo, A. M., Luu, Y. K., Tang, Y., Pessin, J. E., Schwartz, G. J., Czaja, M. J., 2009. Autophagy regulates adipose mass and differentiation in mice. J. Clin. Invest. 119 (11), 3329-3339.

Strappazzon, F., Nazio, F., Corrado, M., Cianfanelli, V., Romagnoli, A., Fimia, G. M., Campello, S., Nardacci, R., Piacentini, M., Campanella, M., Cecconi, F. 2015. AMBRA1 is able to induce mitophagy via LC3 binding, regardless of PARKIN and p62/SQSTM1. Cell Death Differ. *22* (3), 419-432.

Suárez-Zamorano, N., Fabbiano, S., Chevalier, C., Stojanović, O., Colin, D. J., Stevanović, A., Veyrat-Durebex, C., Tarallo, V., Rigo, D., Germain, S. 2015. Microbiota depletion promotes browning of white adipose tissue and reduces obesity. Nat. Med. 21 (12), 1497-1501.

Tanaka, A., Cleland, M. M., Xu, S., Narendra, D. P., Suen, D. F., Karbowski, M., Youle, R. J. 2010. Proteasome and p97 mediate mitophagy and degradation of mitofusins induced by Parkin. J. Cell Biol. 191 (7), 1367-1380.

Taylor, D., Gottlieb, R. A., 2017. Parkin-mediated mitophagy is downregulated in browning of white adipose tissue. Obesity 25 (4), 704-712.

Tseng, Y.-H., Cypess, A. M., Kahn, C. R., 2010. Cellular bioenergetics as a target for obesity therapy. Nat. Rev. Drug Discovery 9 (6), 465-482.

Wang, M.-X., Zhao, X.-J., Chen, T.-Y., Liu, Y.-L., Jiao, R.-Q., Zhang, J.-H., Ma, C.-H., Liu, J.-H., Pan, Y., Kong, L.-D., 2016. Nuciferine alleviates renal injury by inhibiting inflammatory responses in fructose-fed rats. J. Agric. Food. Chem. 64 (42), 7899-7910.

Wang, Z., Cheng, Y., Zeng, M., Wang, Z., Qin, F., Wang, Y., Chen, J., He, Z., 2021.

Lotus (Nelumbo nucifera Gaertn.) leaf: A narrative review of its Phytoconstituents, health benefits and food industry applications. Trends in Food Sci. Tech. 112, 631-650.

Wang, Z., Li, Y., Ma, D., Zeng, M., Wang, Z., Qin, F., Chen, J., Christian, M., He, Z. 2023a. Alkaloids from lotus (Nelumbo nucifera): recent advances in biosynthesis, pharmacokinetics, bioactivity, safety, and industrial applications. Crit. Rev. Food Sci. Nutr. 63(21): 4867-4900.

Wang, Z., Xue, C., Wang, X., Zeng, M., Wang, Z., Chen, Q., Chen, J., Christian, M., He, Z., 2023b. Quercetin 3-O-glucuronide-rich lotus leaf extract promotes a Brown-fat-phenotype in C3H10T1/2 mesenchymal stem cells. Food Res. Int. 163, 112198.

Wang, Z., Xue, C., Yang, T., Zeng, M., Wang, Z., Chen, Q., Chen, J., He, Z., 2023c Miquelianin, a main functional flavonoid of lotus leaf, induces thermogenic signature via p38-PINK1-PARKIN-mediated mitophagy and mimicking NRF2 signaling during brown adipocyte differentiation. Food Frontiers.

Wang, Z., Zeng, M., Wang, Z., Qin, F., Wang, Y., Chen, J., Christian, M., He, Z., 2023d. Food phenolics stimulate adipocyte browning via regulating gut microecology. Crit. Rev. Food Sci. Nutr. 63(19), 4026-4052.

Wu, H., Li, G., Chen, W., Luo, W., Yang, Z., You, Z., Zou, Y., 2022. Drp1 knockdown represses apoptosis of rat retinal endothelial cells by inhibiting mitophagy. Acta Histochem. 124 (1), 151837.

Wu, Z., Du, Z., Tian, Y., Liu, M., Zhu, K., Zhao, Y., Wang, H. 2022)]. Inulin accelerates weight loss in obese mice by regulating gut microbiota and serum metabolites. *Front. Nutr.* 9, 980382.

Xie, S., Li, Y., Teng, W., Du, M., Li, Y., Sun, B., 2019. Liensinine Inhibits Beige Adipocytes Recovering to white Adipocytes through Blocking Mitophagy Flux In Vitro and In Vivo. Nutrients11 (7), 1640.

Xu, Y., Wang, N., Tan, H.-Y., Li, S., Zhang, C., Zhang, Z., Feng, Y. J. T., 2020. Panax notoginseng saponins modulate the gut microbiota to promote thermogenesis and beige adipocyte reconstruction via leptin-mediated AMPKα/STAT3 signaling in diet-induced obesity. Theranostics 10 (24), 11302.

Ye, L.-H., He, X.-X., Yan, M.-Z., Chang, Q. J. A. M., 2014. Identification of in vivo components in rats after oral administration of lotus leaf flavonoids using ultra fast liquid chromatography with tandem mass spectrometry. Anal. Methods 6 (15), 6088-6094.

Yoshida, N., Yamashita, T., Osone, T., Hosooka, T., Shinohara, M., Kitahama, S., Sasaki, K., Sasaki, D., Yoneshiro, T., Suzuki, T., Emoto, T., Saito, Y., Ozawa, G., Hirota, Y., Kitaura, Y., Shimomura, Y., Okamatsu-Ogura, Y., Saito, M., Kondo, A., Kajimura, S., Inagaki, T., Ogawa, W., Yamada, T., Hirata, K.-i., 2021. Bacteroides spp. promotes branched-chain amino acid catabolism in brown fat and inhibits obesity. iScience 24 (11), 103342.

Zhang, M. Y., Zhu, L., Bao, X., Xie, T. H., Cai, J., Zou, J., Wang, W., Gu, S., Li, Y., Li, H. Y., Yao, Y., Wei, T. T., 2022. Inhibition of Drp1 ameliorates diabetic retinopathy by regulating mitochondrial homeostasis. Exp. Eye Res. 220,

109095.

Figure Legends

Fig. 1. Effect of FNE on the beiging in 3T3-L1 cells. (A) Cell viability. (B) qPCR analysis of the mRNA expression of beige fat-related markers. (C and D) Western blot analysis of protein expression of beige fat-related markers. (E and F) Immunofluorescence staining of SIRT1 and UCP1, respectively. Values with different lowercase letters indicate a significant difference at $p<0.05$ according to Duncan's multiple range tests.

Fig. 2. Effects of Q3G on lipolysis and mitochondrial function in 3T3-L1 cells. (A) Chemical structure of Q3G. (B) Cell viability. (C and D) Bodipy/DAPI fluorescent dyes (×200) and fluorescence quantitative analysis. (E and F) Western blot analysis of protein expression of lipolysis-related markers. (G and J) Mitochondrial abundance assessed by Mito-Tracker Red staining. (H and K) Reactive oxygen species (ROS) assessed by DCF-DA assay (×200). (I and L) JC-1 staining and fluorescence quantitative analysis (×200). Values with different lowercase letters indicate a significant difference at $p<0.05$ according to Duncan's multiple range tests. ns indicates no significant differences among groups ($p >= 0.05$).

Fig. 3. Effect of Q3G on the beiging and mitochondrial biogenesis in 3T3-L1 cells. (A) qPCR analysis of mRNA expression of beige fat and mitochondrial biogenesis-related markers (e.g., *Ppargc1α*, *Sirt1*, *Prdm16*, *Cideα*, *Ucp1*, *Pparα*, *Cox7a*, *Cox2*, *Nrf1*, *Tfam*, *Cd40*, *Cd137*, *Cited1*, and *Fgf21*). (B and C) Western blot analysis of protein expression of beige fat and mitochondrial biogenesis-related markers (e.g., SIRT1, PGC-1α, COX-IV, NAMPT, TFAM, and UCP1). (D and E) Immunofluorescence

staining of SIRT1 and UCP1, respectively (×400). (F and G) Western blot analysis of protein expression of β_3-AR, AMPKα, p-AMPKα, AMPKβ_1, p-AMPKβ_1, ACC, and p-ACC. Values with different lowercase letters indicate a significant difference at $p<0.05$ according to Duncan's multiple range tests.

Fig. 4. Effect of Q3G on mitophagy in 3T3-L1 cells. (A) Fluorescence-based images of FCCP (10 μM)-induced mitophagy. (B and C) qPCR ananlysis of mitophagy-related markers (e,g, *Pink1*, *Parkin*, *Beclin1*, *LC-3B*, and *p62*). (D and E) Western blot analysis of protein expression of mitofission marker p-DRP1 and mitophagy-related markers (PINK1, Parkin, p62, Beclin1, and LC-3B). Values with different lowercase letters indicate a significant difference at $p<0.05$ according to Duncan's multiple range tests.

Fig. 5. Effects of Q3G on body weight gain, serum glycolipid levels and tissue histopathology in HFD-fed mice. (A) Body weight was monitored weekly for 12 weeks. (B) Food intake. (C) Liver weight/Body weight. (D) eWAT/Body weight. (E) iWAT/Body weight. (F) TG. (G) TC. (H) LDL-C. (I) HDL-C. (J) FBG. (K-N) H&E staining of eWAT, iWAT, liver, and kidney in different groups. (O and P) Adipocyte size of eWAT and iWAT for each group. (Q) NAFLD activity scores. Values with different lowercase letters indicate a significant difference at $p<0.05$ according to Duncan's multiple range tests.

Fig. 6. Effects of Q3G on the beiging of iWAT in HFD-fed mice. (A) qPCR ananlysis of mRNA expression of beige fat-related markers (e.g., *Sirt1*, *Ppargc1a*, *Prdm16*, *Cideα*, *Ucp1*, *Pparα*, *Cox2*, *Nrf1*, *Tfam*, *Cd40*, *Cd147*, *Cited1*, *Tbx1*, and *Fgf21*). (B)

Immunohistochemistry analysis of SIRT1 and UCP1 in iWAT (200x). (C) Western blot analysis of protein expression of β_3-AR, p-AMPKα, AMPKα, SIRT1, PGC-1α, COX2, TFAM, ABHD5, and UCP1. Values with different lowercase letters indicate a significant difference at $p<0.05$ according to Duncan's multiple range tests.

Fig. 7. Q3G stimulates beiging through blocking AMPK/DRP1-mediated mitophagy. (A and B) Western blot analysis of protein expression of p-DRP1, DRP1, PINK1, PARKIN, BECLIN1, and LC-3B in iWAT of HFD-fed mice. (C) Immunofluorescence analysis for UCP1 (×400) in Q3G-treated cells stimulated with or without Com C or AICAR. (D and E) Western blot analysis of protein expression of p-DRP1, PINK1, PARKIN, BECLIN1, LC-3B, SIRT1, PGC-1α, COX2, and UCP1 in Q3G-treated cells stimulated with or without Com C or AICAR. Values with different lowercase letters indicate a significant difference at $p<0.05$ according to Duncan's multiple range tests.

Fig. 8. Effects of Q3G on the gut microbiota composition in HFD-fed mice. (A) Venn plots. (B) Chao1 index. (C) Shannon index. (D) Non-metric multidimensional scaling (NMDS) analysis. (E) Bacterial taxonomic profiling at the phylum level and the relitive abundances of *Firmicutes* and *Bacteroidetes* and *Firmicutes*/*Bacteroidetes* ratio. (F) Bacterial taxonomic profiling at the family level. (G-I) LEfSe analysis ((1) LDA value distribution histogram; (2) Cladogrsm) of the gut microbiota phylotypes between ND and HFD groups, HFD and Q3G-L groups, HFD and Q3G-H groups, respectively (LDA>3). (J) Heatmap of 20 genera with the highest relative abundance. (K) Spearman’s correlation analysis of these genera and obesity- and beige fat-related

indicators. Values with different lowercase letters indicate a significant difference at $p<0.05$ according to Duncan's multiple range tests.

Fig. 9. Q3G, a main flavonoid in FNE, induces beige-fat formation within WAT *via* blocking AMPK/DRP1/mitophagy signaling and remodeling gut microbiota profiles, thus exerting anti-obesity effects.

Fig. 1

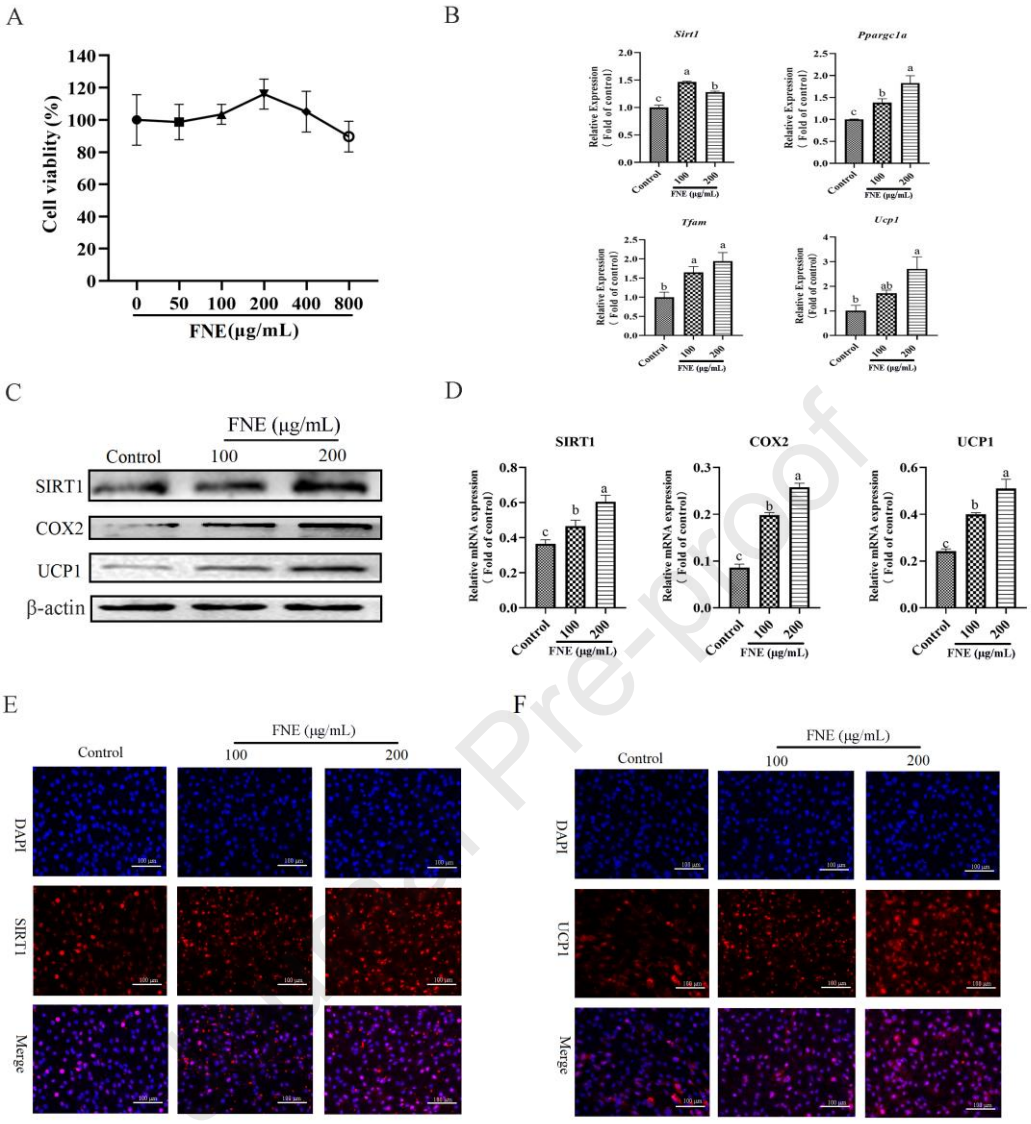
A
Cell viability (%)
FNE(μg/mL)
B
Sirt1
Ppargc1a
Tfam
Ucp1
Relative Expression (Fold of control)
Control
FNE (μg/mL)
C
FNE (μg/mL)
Control
100
200
SIRT1
COX2
UCP1
β-actin
D
SIRT1
COX2
UCP1
Relative mRNA expression (Fold of control)
E
F
DAPI
SIRT1
UCP1
Merge

Fig. 2

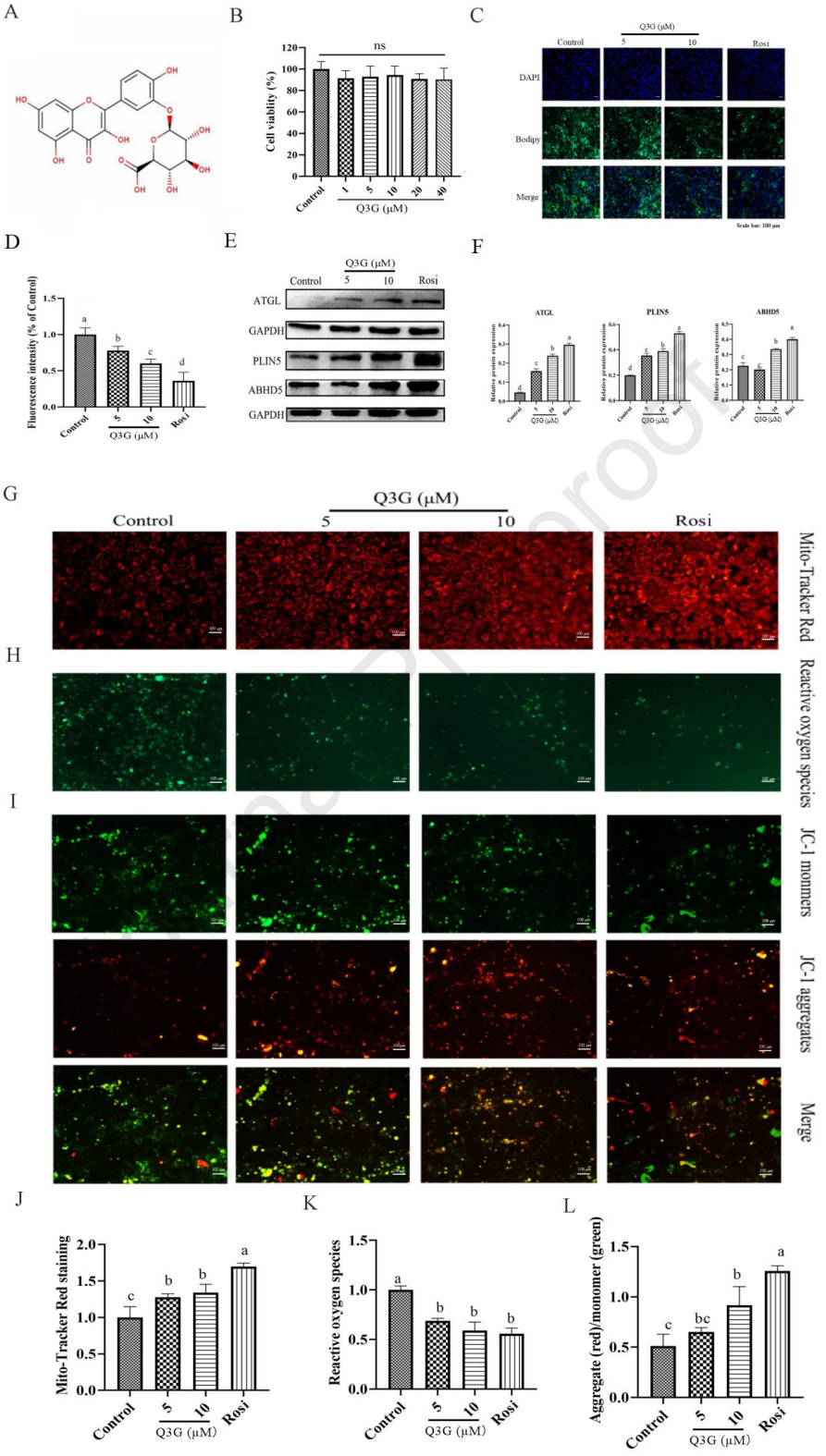
A
B
C
ns
Cell viability (%)
Control
Q3G (μM)
DAPI
Bodipy
Merge
Rosi
D
E
F
Fluorescence intensity (% of Control)
ATGL
GAPDH
PLIN5
ABHD5
G
H
I
Mito-Tracker Red
Reactive oxygen species
JC-1 monmers
JC-1 aggregates
Merge
J
K
L
Mito-Tracker Red staining
Aggregate (red)/monomer (green)

Fig. 3

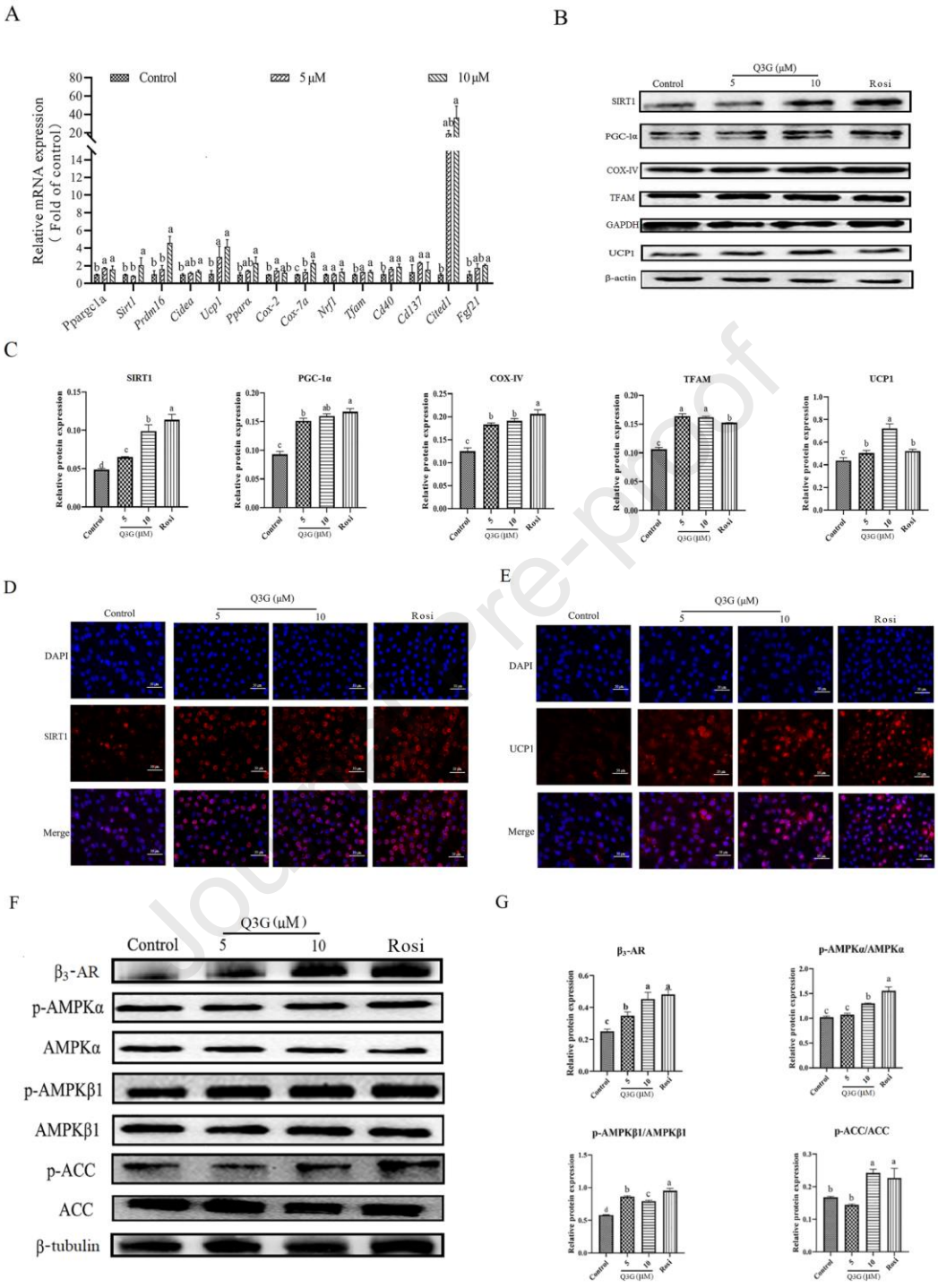

Fig. 4

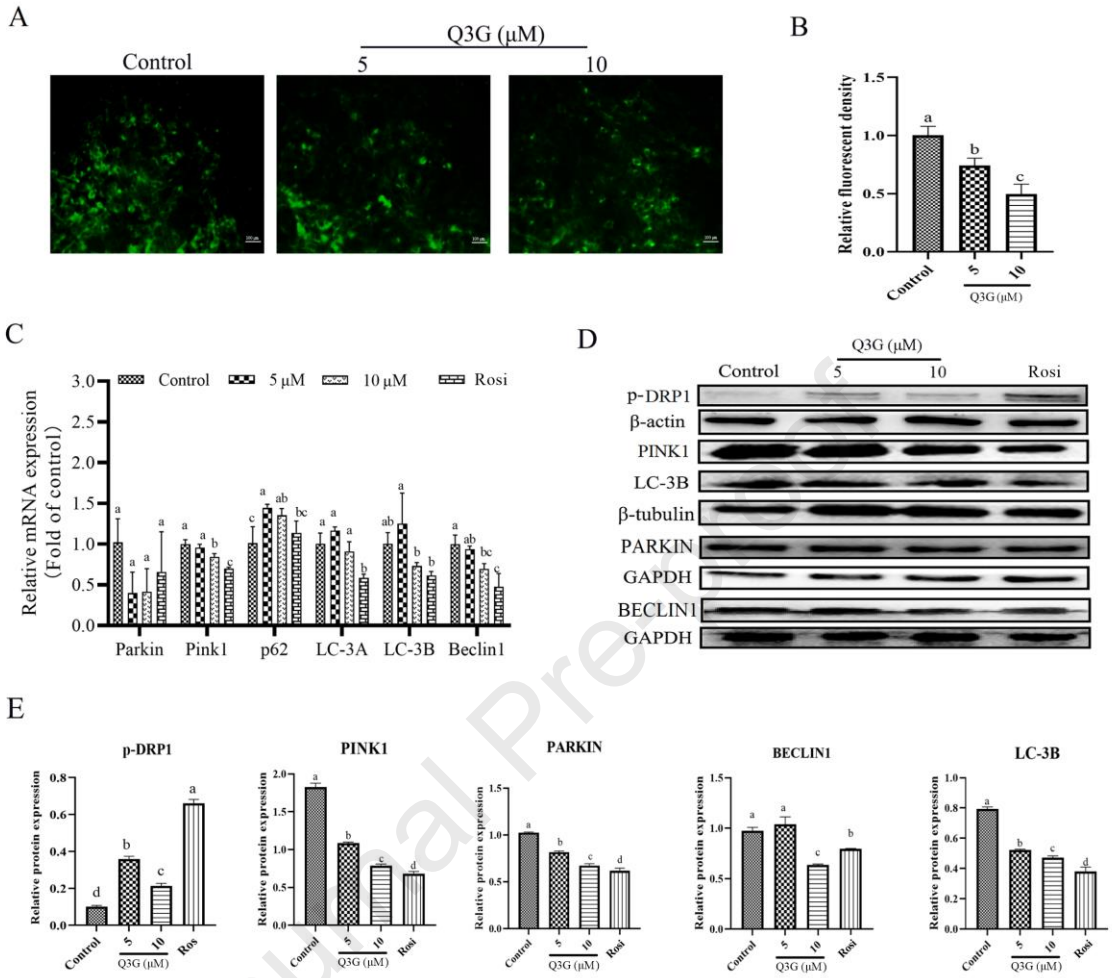

Fig. 5

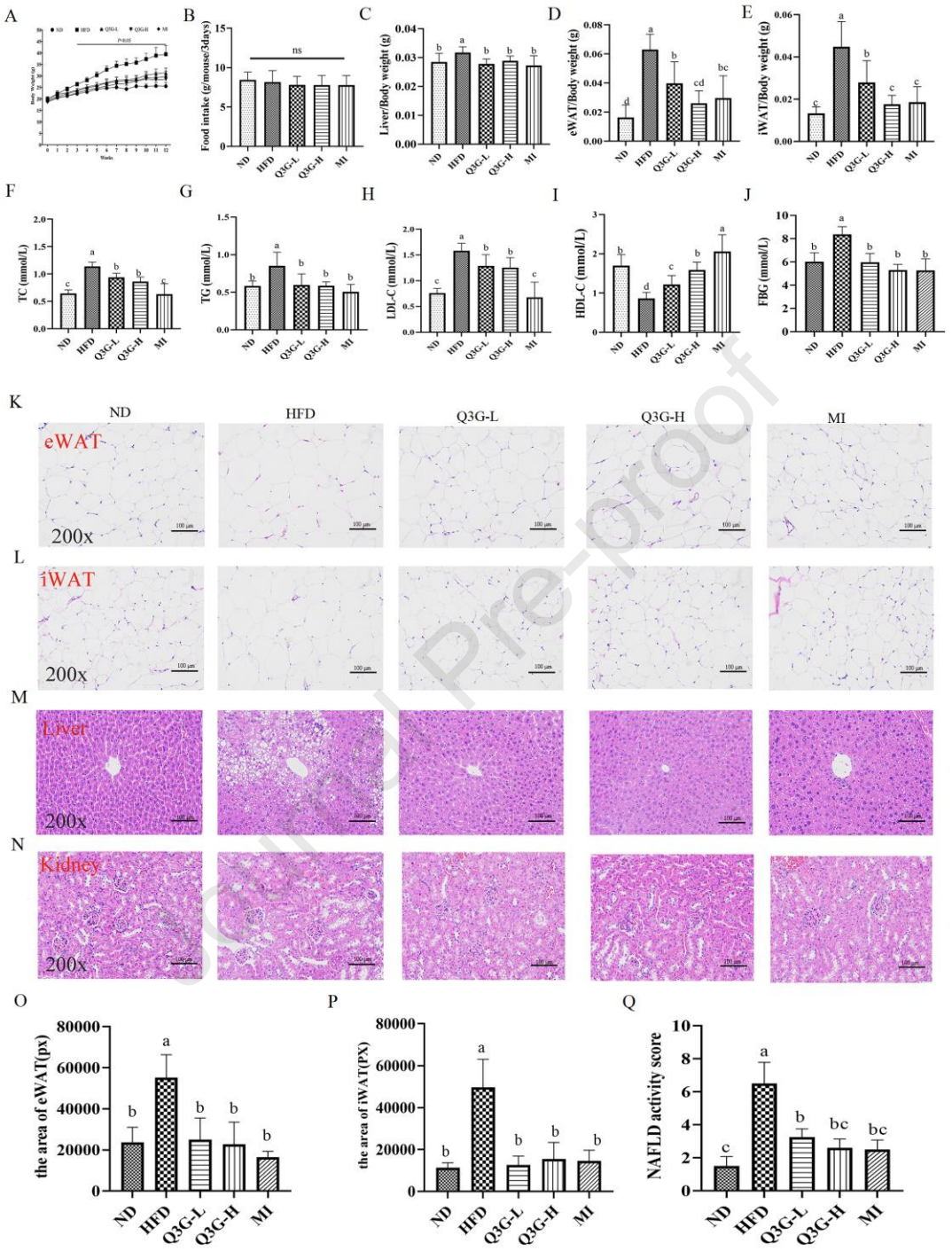
A
B
Food intake (g/mouse/3days)
ns
C
Liver/Body weight (g)
D
eWAT/Body weight (g)
E
iWAT/Body weight (g)
F
TC (mmol/L)
G
TG (mmol/L)
H
LDL-C (mmol/L)
I
HDL-C (mmol/L)
J
FBG (mmol/L)
ND
HFD
Q3G-L
Q3G-H
MI
K
eWAT
200x
L
iWAT
200x
M
Liver
200x
N
Kidney
200x
O
the area of eWAT(px)
P
the area of iWAT(PX)
Q
NAFLD activity score

Fig. 6

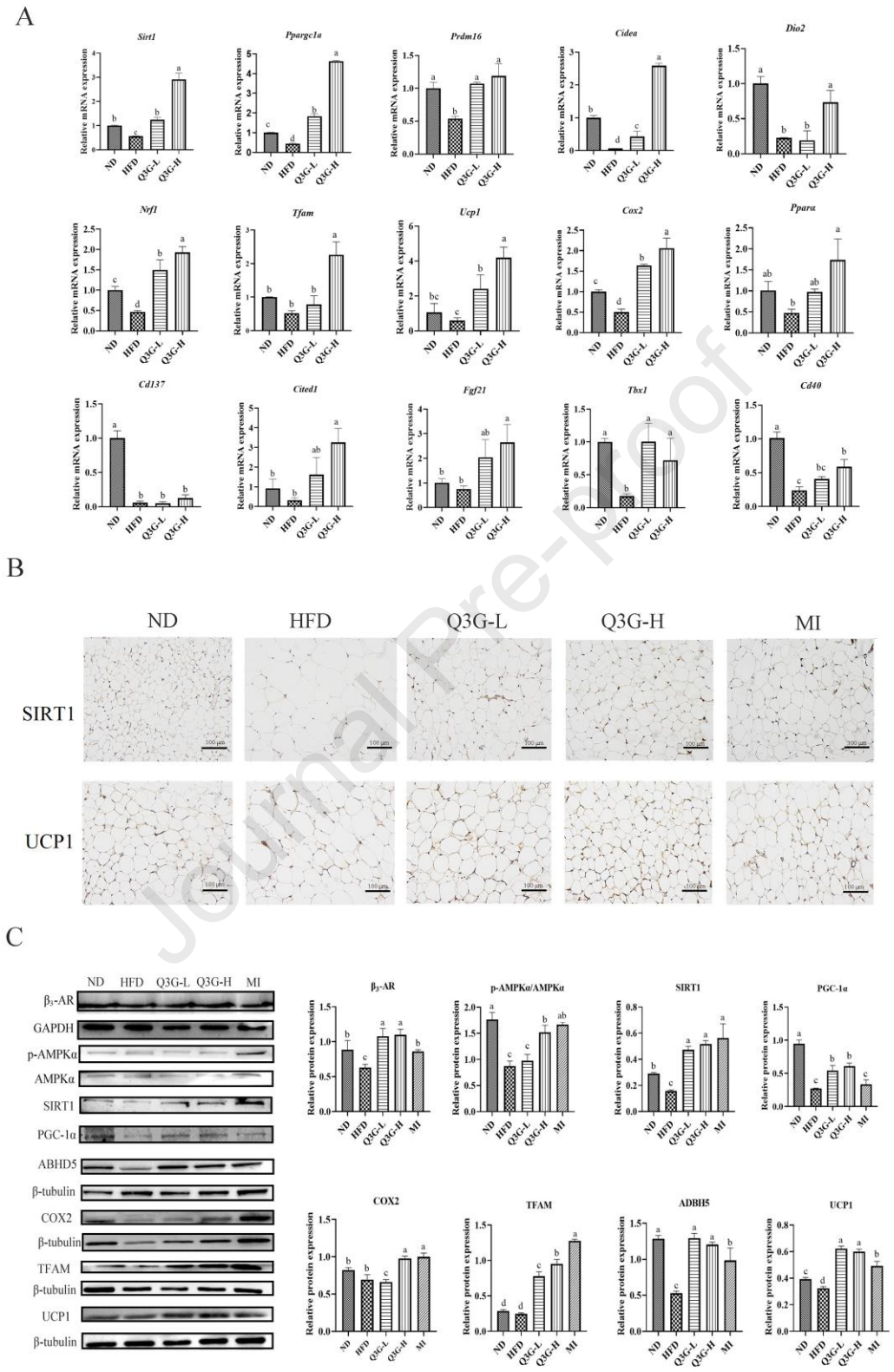

Fig. 7

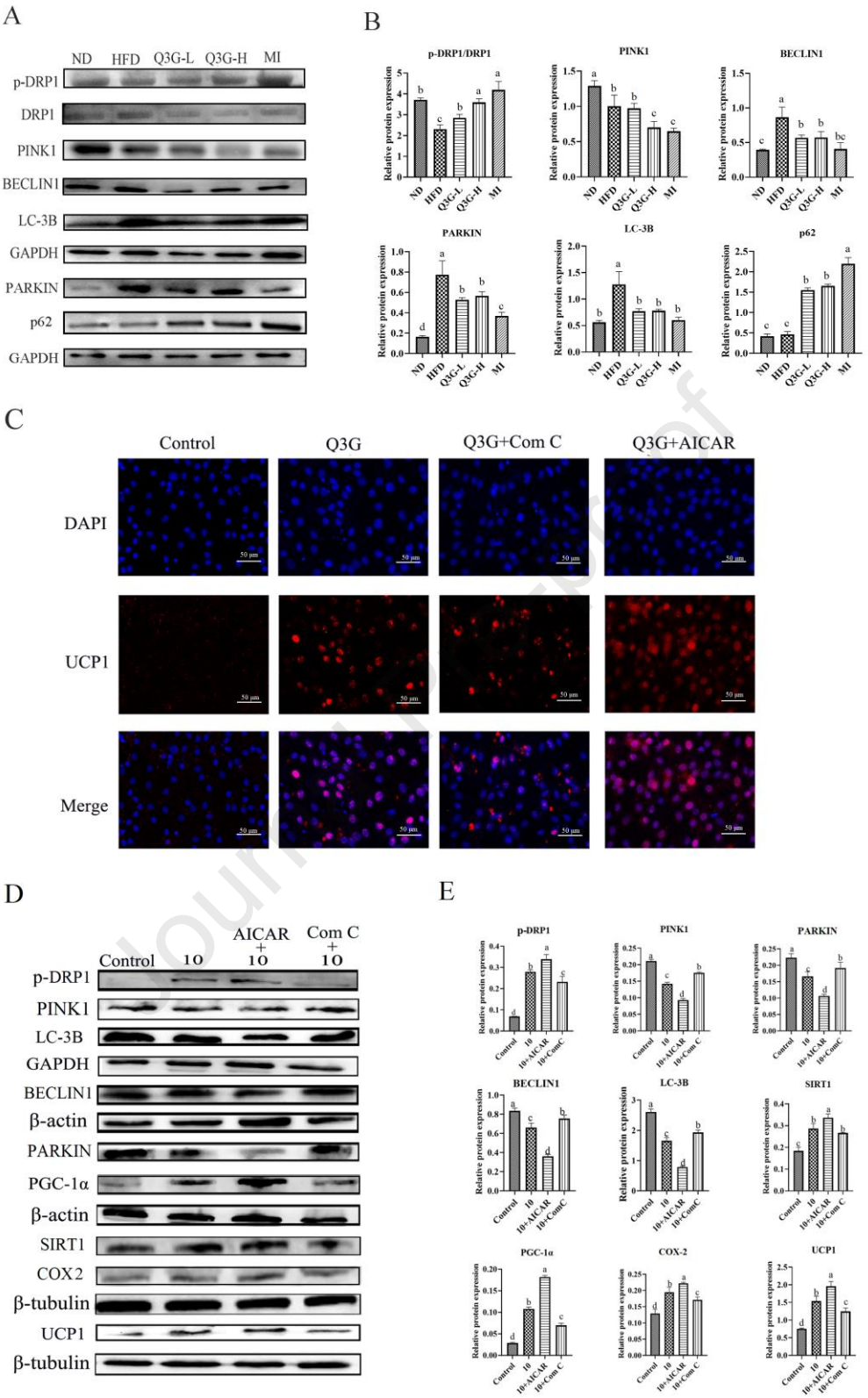
A
ND
HFD
Q3G-L
Q3G-H
MI
p-DRP1
DRP1
PINK1
BECLIN1
LC-3B
GAPDH
PARKIN
p62
GAPDH
B
p-DRP1/DRP1
PINK1
BECLIN1
PARKIN
LC-3B
p62
Relative protein expression
C
Control
Q3G
Q3G+Com C
Q3G+AICAR
DAPI
UCP1
Merge
D
Control
10
AICAR + 10
Com C + 10
p-DRP1
PINK1
LC-3B
GAPDH
BECLIN1
β-actin
PARKIN
PGC-1α
β-actin
SIRT1
COX2
β-tubulin
UCP1
β-tubulin
E
p-DRP1
PINK1
PARKIN
BECLIN1
LC-3B
SIRT1
PGC-1α
COX-2
UCP1
Relative protein expression
Control
10
10+AICAR
10+ComC
10+Com C

Fig. 8

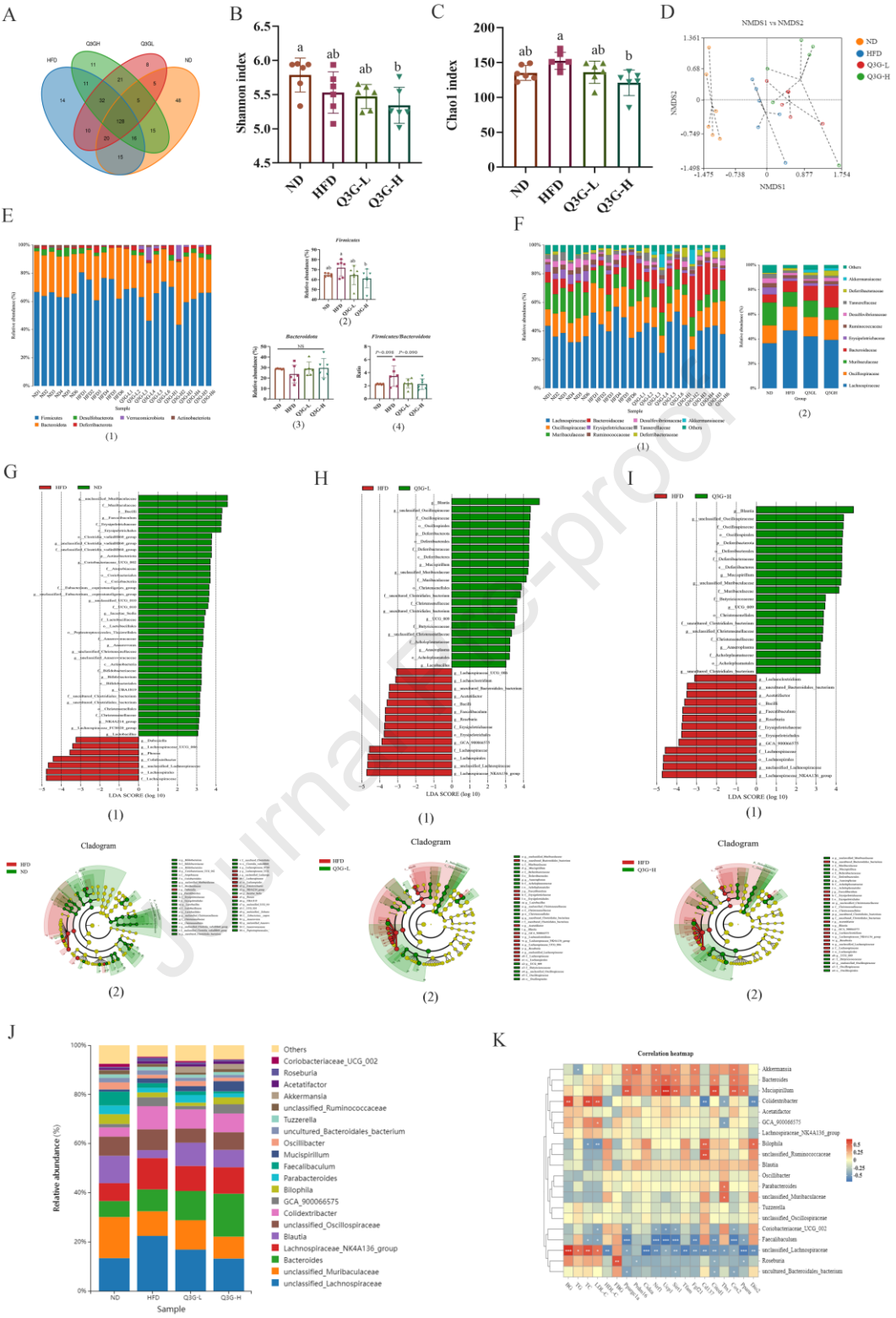

Fig. 9

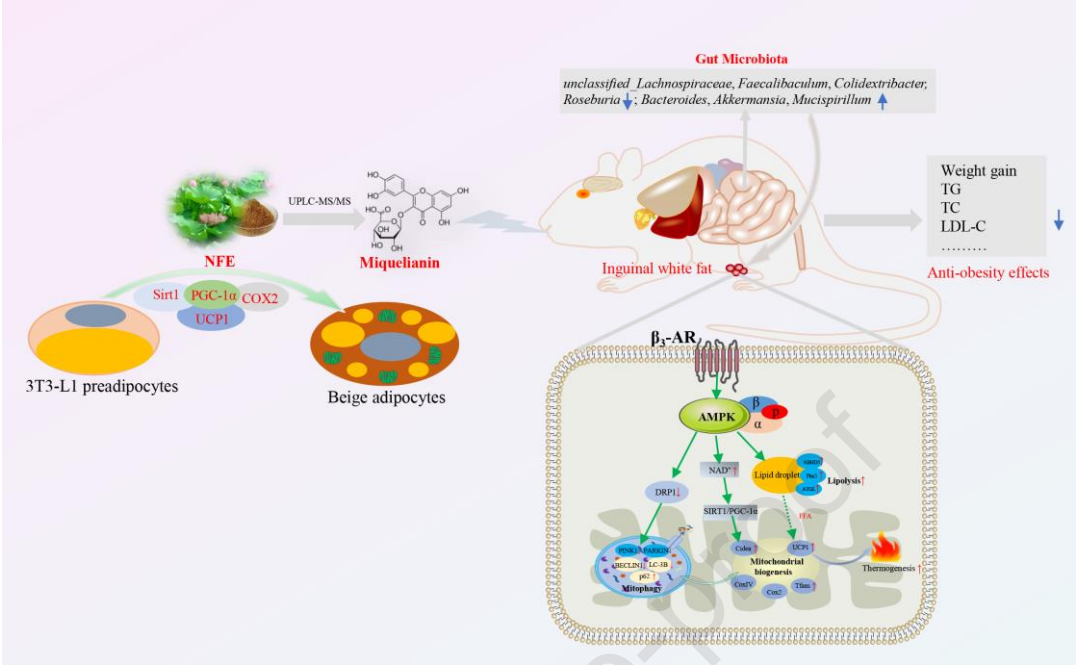

◆Miquelianin-rich *Folium Nelumbinis* extract induces beige-like adipocytes in 3T3-L1 cells.

◆Miquelianin reduces blood glucose/lipid levels and mitigates hepatic steatosis without damage to the kidney.

◆Miquelianin retains beige fat formation by down-regulating AMPK/DRP1/mitophagy.

◆Miquelianin beneficially improves high-fat-diet (HFD)-induced dysbiosis in obese mice.

◆Miquelianin may be an important ingredient in the beige-promoting effects of FNE.

Declaration of interests

☒ The authors declare that they have no known competing financial interests or personal relationships that could have appeared to influence the work reported in this paper.

☐The authors declare the following financial interests/personal relationships which may be considered as potential competing interests: